A.Sierra-Gonzalez, E. Ibarra, I. Kortabarria, E. Trancho and E. Otaola, "REAL-TIME SIMULATION PLATFORM OF AN EMA LANDING GEAR BASED ON MULTIPHASE BLDC," *The 10th International Conference on Power Electronics, Machines and Drives (PEMD 2020)*, 2020, pp. 62-67, doi: 10.1049/icp.2021.1008.

https://doi.org/10.1049/icp.2021.1008

Real-time simulation platform of an EMA landing gear based on multiphase BLDC

A. Sierra-Gonzalez, E. Ibarra†, I. Kortabarria†, E. Trancho*, E. Otaola**

**Tecnalia Research and Innovation, c. Mikeletegi 7, 2009 Donostia (Spain)*
†University of the Basque Country (UPV/EHU), Ingeniero Torres Quevedo 1, 48013 Bilbao (Spain)

Keywords: MEA, EMA, multiphase systems, BLDC, Real-time simulation.

Abstract

Current environmental concerns have led to the partial electrification of the air transport, following the well-known more electric aircraft (MEA) concept. In such aircrafts, electromechanical actuators (EMA) are being progressively introduced to substitute hydraulic actuators. In EMA systems, multiphase technologies are gaining popularity due to their high power density and fault tolerance; however, complexity is increased. In order to accelerate the early development stages of such systems, real-time simulation can be considered. This work presents a real-time simulation platform for a landing gear EMA implemented in an RT-Lab digital simulator, where the multiphase power system is simulated in an FPGA.

1 Introduction

According to the latest International Energy Agency (IEA) report, transport sector is responsible of producing 24 % of world CO_2 emissions [1]. Furthermore, the IEA projects an average annual increase in global transport energy demand of 1.6% between 2007 and 2030. From the total emissions generated by the transport sector, road vehicles are the most significant producer of greenhouse gases with 74% of the total, followed by aviation with 12% of emissions in 2016 [1]. However, air transport has the highest relative increase (115%) of emissions when compared to 1990 levels. Therefore, it is necessary to reduce fuel consumption in aircrafts.

Two load types, i.e., propulsive and non-propulsive, can be distinguished in aircraft. Conventionally, kerosene-powered turbines carry out aircraft propulsion, whereas non-propulsive loads draw pneumatic, mechanic, electric and hydraulic power from burning fuel to run air conditioning, heating, ventilation, fuel pumping, lighting, actuation, etc. In the short and middle term, the electrification of non-propulsive loads is proposed to improve fuel consumption efficiency, weight and volume reduction, control on life-cycle costs, better maintainability, and more reliability and reduced emissions, being this concept named the More Electric Aircraft (MEA) [2,3]. Power electronics and electric machines are core elements in such technology. In electromechanical actuators (EMA), lightweight, efficient and reliable motors are required. These features can be achieved with multiphase permanent magnet motors (PMSM or BLDC) [4,5]. However, these advantages are obtained at the cost of increasing system complexity. Thus, modeling and simulation of multiphase systems becomes more complex than for the conventional three-phase systems [6].

The development of accurate simulation models for such multiphase EMA systems is important to provide a platform for the design and validation of their corresponding controllers during early design stages. Additionally, it is also important to carry out simulations in a variety of operational scenarios such as different load conditions, or fault conditions where the usage of remedial control methods can be tested without putting on risk a physical prototype. In this context, real-time simulation can be considered for the development of such platforms, as this approach allows performing Software-in-the-Loop (SiL) and Hardware-in-the-Loop (HiL) simulations that can be used to accelerate the time-to-market [7].

Considering all these, this paper presents a real-time simulation platform of a complete multiphase landing gear EMA. Such platform has been developed in an OPAL-RT OP4510 simulator, where the controller and the mechanical part of the model have been implemented in a single computational node (CPU) of the real-time simulator, while the electrical domain (power electronics and electric machine) have been modelled in an FPGA using the OPAL-RT eHS solver [8]. This work presents the mathematical basis required for the description of the EMA system, provides details regarding the real-time platform implementation and, finally, presents results, verifying the developed platform.

2 Modelling and control of a multiphase EMA

2.1 Mathematical model of the multiphase BLDC EMA

Two valid approaches for multiphase BLDC modelling can be found in the scientific literature. One common approach consists on using the multiple machine concept, representing an odd phase-number *N*-phase machine into *(N-1)/2* fictitious two phase machines in the synchronous reference frame [6]. However, vector transformations are required in this approach, significantly increasing the implementation complexity when the performance of the power system during faults needs to be

The project leading to these results has received funding from the Clean Sky 2 Joint Undertaking under the European Union's Horizon 2020 research and innovation programme under Grant Agreement no. 755562.

simulated (as the required vector transformations must be modified depending on the phase in which the fault occurs) [9].

The second modelling approach, which is based on the description of the machine model in its natural reference has been followed in this work [5], where the relation between the phase currents and voltages in a multiphase motor is [5]:

$$\mathbf{V} = \mathbf{RI} + \mathbf{L}\frac{d\mathbf{I}}{dt} + \frac{d\mathbf{\Psi}_{PM}}{dt}, \quad (1)$$

where $\mathbf{V} = [v_1, v_2, v_3, v_4, v_5]$ and $\mathbf{I} = [i_1, i_2, i_3, i_4, i_5]$ are the phase voltages and currents. $\mathbf{R} = rI$ is a 5×5 diagonal matrix that represent the phase resistance (I is the identity matrix), $\mathbf{L}$ is a 5×5 matrix which represents the self and mutual inductances, and vector $\mathbf{\Psi}_{PM} = [\Psi_1, \Psi_2, \Psi_3, \Psi_4, \Psi_5]$ represent the per-phase magnetic flux linkages generated by the permanent magnets. In a BLDC machine with trapezoidal back-EMF distribution, the main harmonic components of the flux linkages are the first and third harmonics.

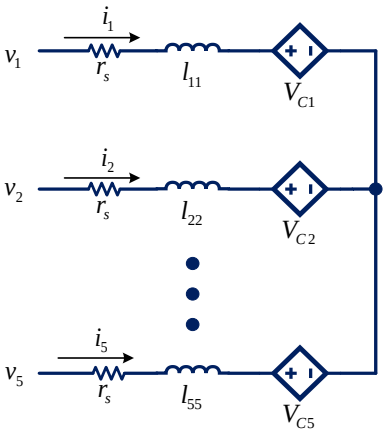

Figure 1: Motor model in the natural reference frame [5].

Figure 1 shows the electrical representation of the 5-phase BLDC motor. The voltage-controlled sources represent the back-EMF and coupling effects, as (2) shows. This way, model implementation in electric circuit simulation software becomes straightforward.

$$V_{Ck} = \frac{d\Psi_k}{dt} + \sum_{j\neq k}^{5} l_{jk}\frac{di_j}{dt}, \quad (2)$$

The electromagnetic torque generated by the motor is:

$$T_{em} = N_p \mathbf{I}^T \frac{d\mathbf{\Psi}_{PM}}{d\theta_e}, \quad (3)$$

where N_p is the pole-pair number. Finally, the mechanical part of the system is represented as:

$$T_{em} - T_l = J\frac{d\omega_m}{dt} + B\omega_m, \quad (4)$$

where T_l is the load torque, J is the moment of inertia of the rotating masses, and B is the viscous friction coefficient of the rotor.

In the landing gear, the motor acts over a ball screw (**¡Error! No se encuentra el origen de la referencia.**). This element transforms the rotational movement of the motor into lineal movement with minimum friction losses. In this work a linear relation between the rotational position of the shaft (θ_m) and the linear position of the actuator (x) is assumed.

2.2 Vector control of the EMA landing gear

¡Error! No se encuentra el origen de la referencia.2 shows the general diagram of the position control of the multiphase EMA landing gear. The control system consists on an outer position loop, responsible for the control of the landing gear linear position. Then, the speed control loop receives the speed reference from the position loop and, using a discrete PI, determines the required electromagnetic torque in each operation instant. The inner torque loop, which is based on the well-known field oriented control (FOC) approach, is adapted to the multiphase scenario, using PI regulators to control the four degrees of freedom of the five-phase BLDC [10]. Such degrees of freedom can be exploited to produce maximum torque per ampere (MTPA) and achieve different objectives depending on the selected injection ratio $r_c = i_{q3}/i_{q1}$ (Table 1) [11].

Objective function	$\max_{r_c} T_{em}$	$\max_{r_c} T_{em}$
Constraint	Same amplitude	Same RMS value
Injection ratio r_c	$\frac{\psi_1}{6\psi_1 - 9\psi_3}$	$\frac{3\psi_3}{\psi_1}$

Table 1: Optimal injection ratio depending the selected constraint.

3 Real-time simulation platform implementation

Figure 3 depicts the general diagram of the real-time EMA landing gear model implemented in an RT-LAB OP4510 digital real-time simulation platform. Such high performance device consists of four computational nodes (an Intel Quad Core at 3.5 GHz), a programmable Xilinx Kintex-7 FPGA 325T (326,000 logic cells, 840 DSP slice), and four I/O boards (32 digital inputs, 32 digital outputs, 16 analog inputs and 16 analog outputs). The hardware synchronized simulation mode has been selected, where real time clocking and synchronization is provided by the FPGA to the rest of computational nodes or CPUs [12]. The distribution of the model elements has been carried out according to their time constants. The controller and the mechanical model have been implemented in one computational node of the PC-cluster of the device (with a sample-time of 10 µs), while the electrical part of the system (power electronics and electric machine) have been modelled in the FPGA (with a sample-time of 250 ns) using the OPAL-RT eHS solver [8]. As the CPU model runs at a low sample-time, firing pulse interpolation (reconstruction) is required in the FPGA. In order to provide

the FPGA model adequate information to reconstruct such firing pulses, the RT-Events toolbox (time stamped signals) [13] has been used.

gear. Figure 4 shows how the speed and position loops regulate the EMA extension following the position command. Figure 5 shows the electromagnetic torque generated by the BLDC

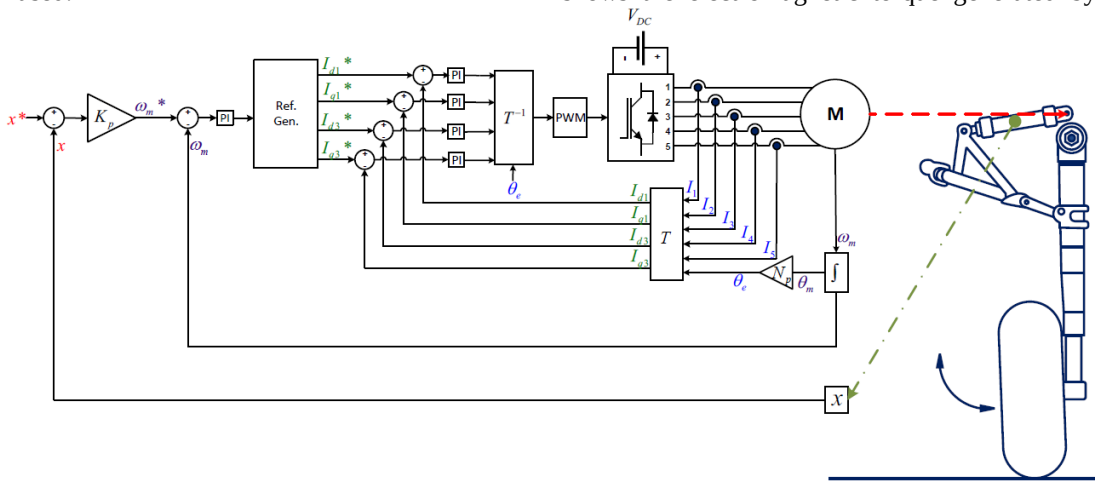

Figure 2 General diagram of the position control of the landing gear EMA during normal operation.

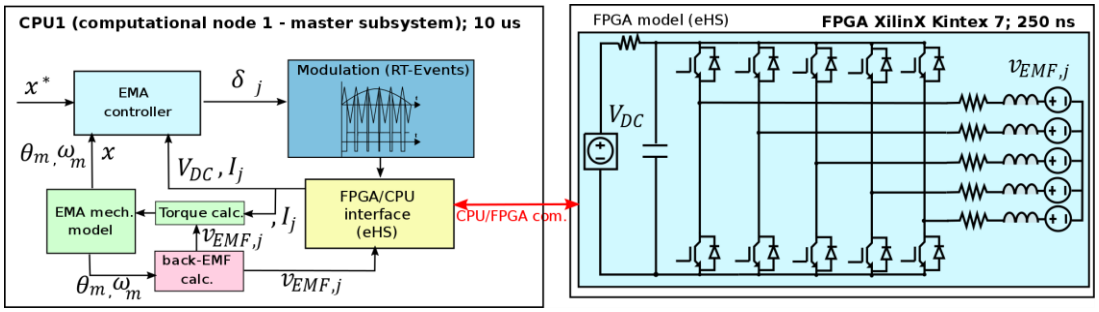

Figure 3 General diagram of the implemented Real-time multiphase EMA landing gear platform in OP4510.

4 Results

In order to validate the proposed real-time model, SiL simulations have been carried out for an EMA landing gear. Table 2 summarizes its most significant parameters.

Parameter	*Symbol*	*Value*
Stator inductance	L_s	9.6 mH
Stator resistance	R_s	1.56 Ohm
First harmonic PM flux	ψ_1	0.1314 Wb
Third harmonic PM flux	ψ_3	0.0293 Wb
Rated power	P_N	1.51 kW
Rated torque	T_N	12.1 Nm
Rated speed	ω_N	1200 RPM
Pole pair number	N_p	9

Table 2: Most relevant parameters of the multiphase BLDC and EMA landing gear.

The following figures show the most significant results obtained in real-time during an extension of the EMA landing

machine during extension. The multiphase machine degrees of freedom ($i_{d1}, i_{q1}, i_{d3}, i_{q3}$) have been commanded to achieve MTPA operation while keeping the same RMS value in the phase currents (Figures 6 and 7), operating as expected.

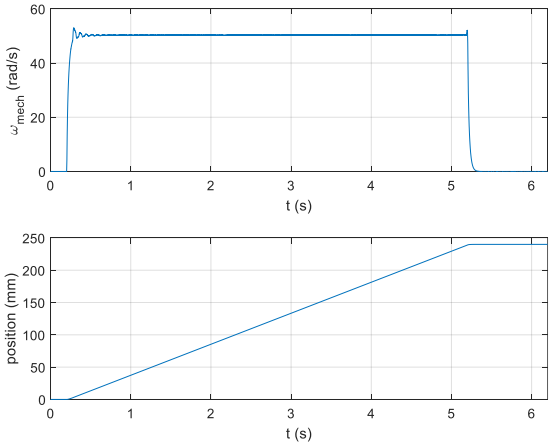

Figure 4: Speed and position control during the EMA landing gear extension.

5 Conclusions

In this paper, a real-time simulation platform for multiphase BLDC EMA landing gears has been proposed and validated.

The usage of natural variables instead of vector transformations for the machine modelling has simplified the implementation of the real-time model.

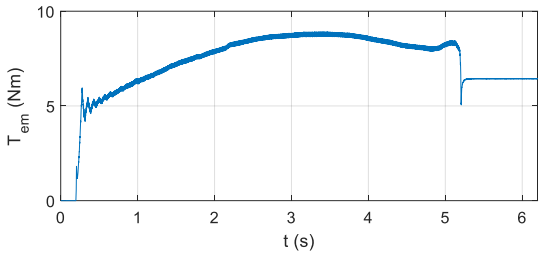

Figure 5: Electromagnetic torque produced by the fundamental and third harmonic components.

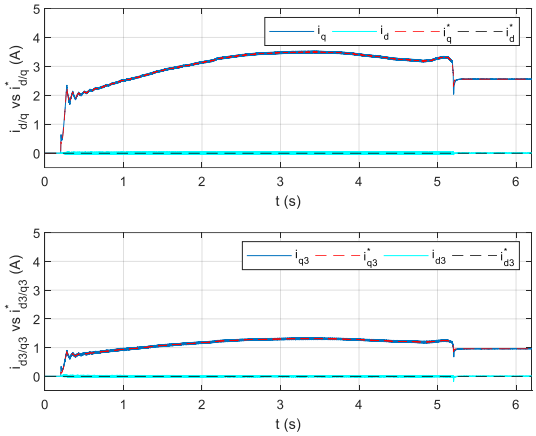

Figure 6: Fundamental and third harmonic d- and q-axis current control.

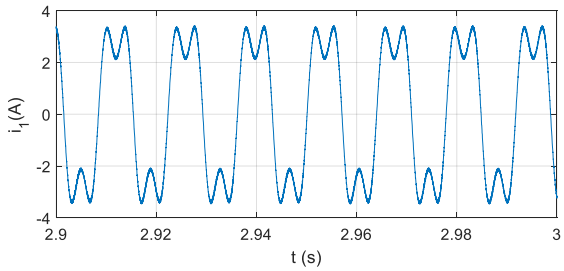

Figure 7: Phase U current during maximum load conditions.

The model has been validated in SiL. Physical HiL has not been carried out at this development stage. However, its implementation can be straightforward. For that purpose, the controller model must be removed from the CPU. Finally, various signals must be routed through the I/O boards. Resolver *sin* and *cos* signals and power system DC link voltage and stator currents must be sent using the analog outputs board of the RT-Lab. The resolver excitation signal must be received in the analog inputs board, and PWM signals must be sent back from the physical controller to the digital inputs board to feed the virtual FPGA power converter.

References

[1] IEA, CO2 Emissions from Fuel Combustion 2018, Tech report, OECD, (2018).

[2] P. W. Wheeler, J. C. Clare, A. Trentin, S. Bozhko, “An overview of the more electrical aircraft,” Journal of Aerospace Engineering, vol. 227, pp. 578–585, (2012).

[3] W. Cao, B. C. Mecrow, G. J. Atkinson, J. W. Bennett, and D. J. Atkinson, “Overview of electric motor technologies used for more electric aircraft (MEA),” IEEE Transactions on Industrial Electronics, vol. 59, pp. 3523–3531, (2012).

[4] J. Karttunen, S. Kallio, P. Peltoniemi, P. Silventoinen, O. Pyrhönen, “Decoupled vector control scheme for dual three-phase permanent magnet synchronous machines”, IEEE Transactions on Industrial Electronics, Vol. 61, pp. 2185-2196, (2014).

[5] A. Sierra, E. Ibarra, I. Kortabarria, J. Andreu, J. Lasa, “Evaluation of the intrinsic fault tolerance of an EMA landing gear based on a five-phase SM-PMSM”, in Proc. of the More Electric Aircraft Conference (MEA), pp. 1-4, (2019).

[6] E. Semail, A. Bouscayrol, J.P. Hautier, “Vectorial formalism for analysis and design of polyphase synchronous machines,” The European Physical Journal Applied Physics vol, 22(3), pp. 207–220, (2003).

[7] V.I. Herrera, A. Milo, H. Gaztañaga, A. González-Garrido, H. Camblong, A. Sierra-Gonzalez, “Design and Experimental Comparison of Energy Management Strategies for Hybrid Electric Buses Based on Test-Bench Simulation”, IEEE Transactions on Industrial Applications, vol. 55(3), pp. 3066-3075, (2018).

[8] J. Belanger, A. Yamane, A. Yen, S. Cense, P. Robert, “Validation of eHS FPGA reconfigurable low-latency electric and power electronic circuit solver,” in Proc. of the IEEE Industrial Electronics Society Conference (IECON), pp. 5418–5423, (2013).

[9] H.M. Ryu, J.W. Kim, S.K. Sul, “Synchronous-frame current control of multiphase synchronous motor under asymmetric fault condition due to open phases,” IEEE Transactions on Industry Applications, vol. 42(4), pp. 1062-1070, (2006).

[10] L. Parsa, H. Toliyat, “Five-phase permanent-magnet motor drives,” IEEE Transactions on Industry Applications, vol. 51(1), pp. 30-37, (2005).

[11] Y. Sui, P. Zheng, Y. Fan, J. Zhao, “Research on the vector control strategy of five-phase permanent-magnet synchronous machine based on third-harmonic current injection," in Proc. of the International Electric Machines and Drives Conference, pp. 1-8,(2017).

[12] H. Chen, C. Gan, B. Xia, P. Rafajdus, “RT-Lab simulator for simulation of switched reluctance machine,” in Proc. of the IEEE International Symposium on Industrial Electronic, pp. 737–741, (2012).

[13] A. Bouzid, P. Sicard, S. Abourida, J. Paquin, “Secondary voltage and frequency restoration control of droop-controlled inverter-based microgrids,” in Proc. of the IEEE-GCC Conference and Exhibition, pp. 1–6, (2017).